2mip

ATS-16890

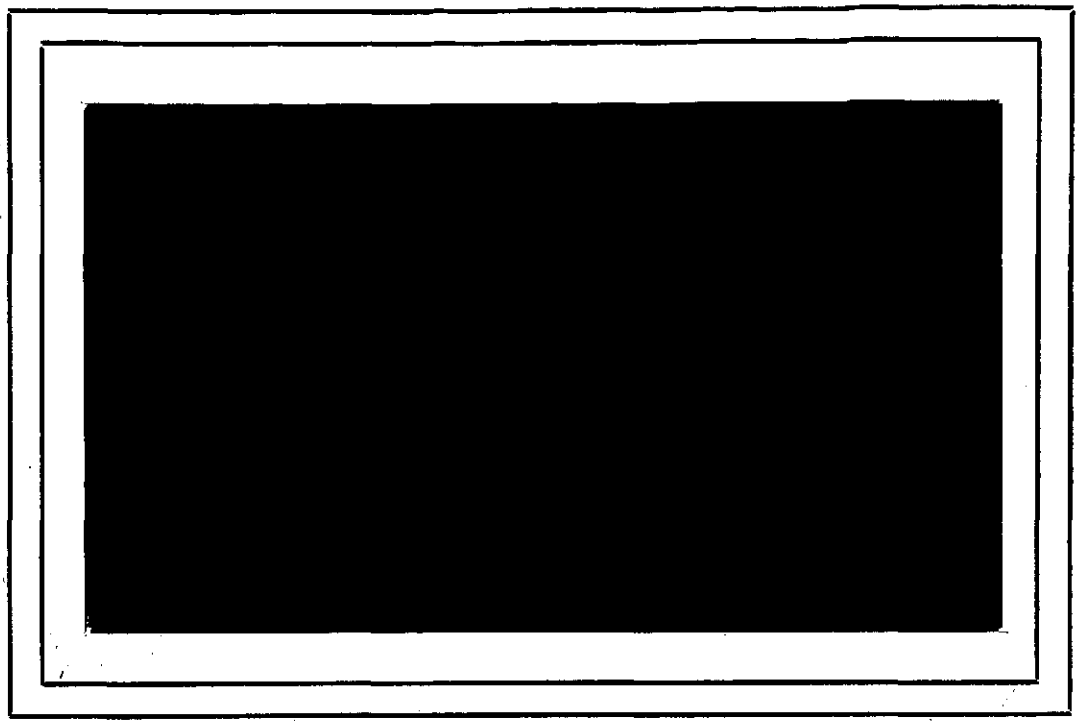

UNIVERSITY OF MARYLAND
COMPUTER SCIENCE CENTER

COLLEGE PARK, MARYLAND

Technical Report TR-285 January 1974
NGR 21-002-351

A QUANTITATIVE STUDY OF THE ORIENTATION BIAS OF SOME EDGE DETECTOR SCHEMES

By
J. R. Fram
and
E. S. Deutsch

ABSTRACT

Further work on the evaluation of a particular set of edge detection schemes is described. The results obtained are compared with those obtained from an edge detection scheme using a texture oriented approach. The orientational bias of these schemes is addressed in particular. Improved qualitative observations are reported and a comparison of the evaluation method discussed here with another edge detection evaluation method is presented.

The support of the National Aeronautics and Space Administration under Grant NGR 21-002-351 is gratefully acknowledged.

1. INTRODUCTION

Image segmentation techniques by means of edge detection methods bound in the literature. Previous work in the same area, reported upon by the authors in [1], concentrated largely upon the proposal of parameters which could lead to a quantified evaluation of such methods. Initial experimental results using the parameters proposed, as well as their comparison with human evaluation, were reported. These evaluation experiments were made using a set of generated edge-containing images containing different contrast and noise values. The edges contained in these images were located vertically along the center of the images. The behavior of these parameters using edge orientations other than in the vertical direction were not discussed and is reported upon here. The method employed here to quantitatively evaluate edge detection performance is compared with a method due to Herskovits and Binford [8].

A potential drawback of the three schemes evaluated thus far is that the edge finds are not constrained to be continuous. After applying one of these edge detection schemes to an image it is necessary to apply some post processing to the resulting edges in order to join smaller edge lengths to form a continuous edge and also in order to eliminate spurious short edge lengths. An edge

finding method whose output consists of continuous edges, closed where appropriate, is described and is presented for the sake of comparison. It has the advantage that little post processing is required since the nature of its operation ensures that no 'loose' edges are generated to start with. The method uses a simple 'difference test' based upon the grey level of a group of image picture points and defines like-areas by means of a 'blob' aggregate technique. The investigation of such an approach was prompted by work reported by Muerle in [2]. While the work to be described employs a simpler test than that reported in [2] it employs a considerable amount of 'backtracking' (a term whose use will be clear later), a feature not used in [2] at all.

2. BLOB AGGREGATE METHOD

2.1 Description.

The image is subdivided into small subsquares of size d x d and a new image is constructed such that the grey level of the points in each subsquare is equal to the mean of the grey levels of the points in the original image within the same area. Subsquares are considered to be similar, that is, belonging to the same region within the original image, if their associated grey level difference does not exceed a given value μ. The segmentation algorithm thus consists of combining 'similar' subsquares, deemed to form a single region, and relegating 'dissimilar' subsquares to a new region. It is then a simple matter to isolate the specific regions so found, or, for visual purposes, place a boundary between the regions. Given this approach, the two variables effecting the performance are d and μ.

The above approach is by no means novel; however, to the authors' knowledge [3], a feature not considered hitherto is the effect further combination of already combined subsquares has. For once a set of subsquares has been combined it is necessary to recalculate their new mean before proceeding to the next subsquare, a feature involving not inconsiderable backtracking if this is to be done in 2 dimensions equally. Muerle [2], using the difference between the

cumulative distribution of the grey levels in the subsquares combined so far and the cumulative distribution of the grey levels in the subsquare under consideration (grey level values are not averaged, the image being subdivided into a simple grid of subsquares) allowed this difference to vary as the number of combined subsquares increased, thus avoiding reprocessing. The approach here was to strike a possible balance between the need for reprocessing on the one hand and the cost involved in recomputing differences of cumulative distributions on the other.

In a sense, the use of the averaged subsquares method rather than the cumulative distribution approach might seem more advantageous in view of the type of images used. In an image in which the grey level change is fairly high, the cumulative approach may be superior since it relies upon the individual statistics of the grey levels within each subsquare. Where the image is changing at a fairly low rate (such as those used here) calculations of distributions may not be very useful and the mean grey level might as well be used.

Given an N x N image, reconstructed in terms of subsquares as described above, the number of subsquares is given by $\frac{N}{d} \times \frac{N}{d}$. Let the subsquare on each row or column be re-

ferred to in the usual matrix notation, so that any subsquare is identifiable as $S_{i,j}$, $1 \leq i \leq \frac{N}{d}$, $1 \leq j \leq \frac{N}{d}$. Starting with the first row of subsquares, subsquare $S_{1,1}$ is arbitrarily assigned to constitute the first region. Next, $S_{1,1}$ and $S_{1,2}$ are examined and provided their associated grey level values differ by an amount not exceeding μ, $S_{1,1}$ and $S_{1,2}$ are said to belong to the same region and are hence combined. A new mean, based upon the combined subsquares' grey levels is computed and $S_{1,3}$ examined and so on until $S_{1,\frac{N}{d}}$. Should the grey level differences of $S_{1,j}$ and $S_{1,j+1}$ exceed μ, they are then said to belong to two different regions and a vertical boundary separating them can be tentatively placed between them.

In processing subsequent rows, the following steps are taken at $A_{i,j}$: subsquare $S_{i,j}$ is compared with subsquare $S_{i-1,j}$, on the previous row. If $S_{i,j}$ and $S_{i-1,j}$ are similar, $S_{i,j}$ is associated with the region encompassing $S_{i-1,j}$ and a new mean relevant to this region is calculated. A check is made to establish whether subsquare $S_{i,j-1}$ is assigned to any other region; if it is then no merging of $S_{i,j-1}$ is performed and the next subsquare to be considered is $S_{i,j+1}$. Should $S_{i,j-1}$ constitute a single-subsquare region an attempt at combining $S_{i,j-1}$ with the region to which $S_{i,j}$ belongs is made. Should such a combination fail $S_{i,j+1}$ is considered next, otherwise $S_{i,j}$ and $S_{i,j-1}$

are merged and $S_{i,j-2}$ examined, just as $S_{i,j-1}$ was, to establish whether it belong to the region consisting of among other subsquares $S_{i,j}$ and $S_{i,j-1}$. This row backtracking terminates either when a non single subsquare region on the row is located (i.e. a subsquare already belonging to a region is encountered) or when merging ceases by virtue of dissimilarity. Should no row merging or backtracking have been initiated at all, (i.e. $S_{i,j}$ and $S_{i-1,j}$ were dissimilar) $S_{i,j+1}$ is considered next and so on.

Upon the termination of row backtracking at $S_{i,\frac{N}{d}}$, a new backtracking is initiated. Here all $S_{i,j}$ subsquares, on the current row, which have not been merged with an already existing region are examined. At first they each are treated as a subsquare forming a new region; however, an attempt is made to combine each $S_{i,j}$ with its $S_{i,j-1}$ neighbor. Should such a combination occur a new mean is calculated for both and $S_{i,j-2}$ is considered and so on. Once $S_{i,j}$ and $S_{i,j-1}$ are combined their associated mean is checked against that associated with $S_{i-1,j}$ and the latter subsquare combined with $S_{i,j}$ and $S_{i,j-1}$ if possible.

2.2 Results.

Figure 1 shows some of the results obtained using various values of d and α with three different ERTS satellite images. The edges found have been superimposed on the images themselves. An immediately apparent feature of this scheme is the step-like nature of the edge contours. This is to be expected in view of the rectangular shape of the subareas used. Furthermore, the fact that the top-left edge point at the confluence of a vertical and horizontal edge is missing is due to the edge placement routine and follows directly from the way edges are inserted between neighboring subsquares.

Where the objects are well defined with respect to the background the method works reasonably well and appears to give results very similar to those shown in [2]. Line detail seems to be missed however and would thus suggest a limitation of this approach. 'Blob growing' has been applied to multispectral imagery [4], with a degree of success, but it should be borne in mind that the type of imagery used there is of a different structure. For unlike the scenes of Figure 1, the imagery consisted of near-rectangular different agricultural fields bordering on one another; a pattern which would be admirably suited for

this kind of approach. It is questionable whether this method would work equally well with imagery containing more subtle detail. The results shown in Figure 1* should be compared with those shown in Figure 2, which shows the output obtained from the three schemes of [1]. Here too some post processing is required to eliminate spuriously found blobs.

In terms of operation time, the method described above is twice as fast as that described in [2], but is almost a magnitude of time slower than the longest of the three edge detection methods discussed in [1]. The latter are now discussed again in the next section.

*The imagery was taken from an ERTS satellite picture over the Monterey region.

3. A QUANTITATIVE ASSESSMENT OF THE ORIENTATION BIASES OF SOME EDGE DETECTION SCHEMES

3.1 Background.

A method for quantitatively comparing the performance of edge detection programs in the presence of noise was presented in [1]. Under this method, standard sized test images with vertical edges and pseudo-random noise were generated by computer with various ratios of contrast to noise. The output of several edge detectors operating on the test images was then processed in such a manner as to yield two parameters reflective of each edge detector's performance on each test image. The average values of the two parameters for each edge detector over each subset of test images of a given ratio of contrast to noise were indicators of the performance of the edge detection scheme. The average value of the first parameter characterized the freeness from noise of the edge detector output or more accurately, the fraction of this output which was signal. The average value of the second parameter characterized the distribution of the output over the length of the edge. Both parameters had maximum probability values of 1 for ideal performance and values of 0 for random output.

Three types of edge detectors were evaluated by the above procedure.

1. The local visual operator due to Hueckel [5] under which the gray level values from disk-like areas of the image containing, in this case 69 picture points, were analytically fit to the member of a set of ideal edge-lines whose gaussian error of approximation to the original disk was minimum. If the results of this fit indicated the likely presence of an edge or line running through the disk, then the edge or line strength was returned along with its orientation. Only the edge-information of this method was evaluated in [1]. The line information was not considered.

2. The gaussian edge mask detector due to Macleod [6]. Under this scheme, edge weights were computed for each point by multiplying the gray level value of each point in a surrounding neighborhood by the value of the corresponding point of a mask and summing. The mask consisted of the difference of two gaussians displaced perpendicular to the expected edge direction multiplied by a gaussian envelope which tapered off parallel to the expected edge direction. This mask was given by

$$w(x,y) = e^{-\left(\frac{y}{t}\right)^2}\left[e^{-\left(\frac{x-p}{p}\right)^2} - e^{-\left(\frac{x+p}{p}\right)^2}\right]$$

for edges expected to be in the vertical direction. The absolute values of the resulting edge weights were used in [1]

to assess the performance of this scheme. Two sizes of the above mask were used--one with $p = t = 4$ inside a 7 x 7 square and $w(x,y) = 0$ outside and one with $p = 4.7$ and $t = 4$ inside a 13 x 13 square and $w(x,y) = 0$ outside.

3. The local difference calculations due to Rosenfeld [7]. Here the edge weight assigned to each point was the difference in average grey level of two squares adjacent to the anticipated edge. The side of the squares could be any power of two and four optimum orientations were available. In [1], 8 x 8 squares were used with a vertical optimum orientation. An algorithm for non-maximum suppression also due to Rosenfeld was evaluated as well.

As was pointed out in [1],(Section 5.1), the work there was incomplete in the sense that the orientation biases of the methods due to Macleod and Rosenfeld were not properly taken into account. The method due to Hueckel could be expected to be free of orientation biases but the other two were clearly not. The assumption was made, without proof, that two optimum orientations were sufficient to effectively remove the biases from the other two methods. In this work, the question of orientation biases is addressed directly. Also, a comparison of our method of evaluating edge detectors is made with that described by Herskovitz [8].

In the present work, the performance of the three edge detection schemes evaluated in [1] for the vertical orientation is studied at skew orientations. The following changes were made, however, in the implementation of these schemes:

1. It was discovered after publication of [1] that the application density of the operator due to Hueckel was slightly less than that recommended in [5]. Here the application pattern used was identical to that of [5],(Figure 5), save that edges so found were not followed as indicated there. The resulting differences, however, in the ratings of this scheme were small.

2. Because, in our implementation, the larger mask required increased computer time,only the smaller mask of the scheme due to Macleod was used in this work.

3. In [1], the output of Rosenfeld's method,in which non-maxima were suppressed,consisted only of the edge weights for which the "best" orientation was vertical. Here, both the vertical "best" orientation output and the horizontal "best" orientation output were used. The edge weight used was the greater of these two at each point. There were two reasons for this change:

1. The two-orientation approach described above was the more natural implementation for most applications.

2. At the larger angles, much of the edge information was channeled into the horizontal "best" orientation output. Were only the vertical "best" orientation output considered, the ratings would have indicated a poorer performance than was actually obtained.

3.2 Generalization of the Parameters to Arbitrary Orientations.

In principle, the question of orientation biases could be investigated either by rotating the test images or changing the optimum orientation of the edge detectors. In practice, however, the former of these was the more convenient and reliable. Though rotating test images introduced distortions, it was a well-defined conventional operation which did not appear to bias the results. In contrast, rotating Rosenfeld's edge detector, for example, was not at all well defined, and no good test of Hueckel's operator for hidden orientation biases (which were not found) could be devised other than rotating the test images.

Four sets of test images were generated to the same specifications of the test images used in [1]. These were rotated by 15^{o}, 30^{o}, 45^{o}, and 60^{o} (See Table 1). The 60^{o} orientation might seem to be unnecessary because the edge

detectors investigated could be readily rotated* by 90°, and the original detector plus the 90°-rotated version together would form the minimum set one could hope to use for arbitrarily oriented edges. But in such a case, the greatest angle an edge could make with an optimum orientation would be 45°. The 60° orientation was included nevertheless since it indicates how rapidly the performance drops beyond the 45° orientation.

In evaluating the edge detectors' performance on the rotated edges, we were faced with a decision analogous to the one discussed in the beginning of this section, i.e. whether to rotate the edge detector output back so that the edge region was again vertical or to redefine the two parameters in such a manner that they reduced to the original parameters (in the case of vertical edges) and had the same significance for the rotated edges as they did for the unrotated ones. The former approach was adopted because: (a) it was difficult to define parameter 2 in a rotationally invariant manner and (b) rotating the picture back provided a convenient means to eliminate possibly questionable information content. The following illustrates the argument for

*Indeed, it would appear from the symmetry of the rectangular coordinates used that any edge detector defined in these coordinates would possess this property.

(b). Consider a square image with a straight edge passing through the center oriented 45^{o} to the vertical. In general, one would expect the performance of edge detectors to be poorer at the corners of the image through which the edge passes because there information from points removed from the edge in a direction perpendicular to it is not available. Rotating the edge detector output back so that the edge is vertical, however, rotates these points out of the image. In general, the effects of the boundary are larger in the test images than they would be in most applications because the test images are small. It is desirable, therefore, in a quantitative evaluation of edge detector performance to minimize such effects.

Thresholding the edge detector output was performed after it was rotated back so that the edge region was vertical. As was done for vertical edges, the threshold was determined for each test image to permit enough points to pass to fill the edge region [9]. A difference between the rotated-edge output from the vertical-edge output was that the former contained a greater proportion of points in the edge region than did the latter. Compensation was made for the effect of this on the threshold determination by weighting the points

inside and outside the edge region separately in such a manner that the rotated-edge output effectively had the same fraction of points inside the edge region and the same total number of points as did the vertical-edge output. As in [1], the number of points in the threshold determination which were considered to fill the edge region, n_{fill}, varied from detector to detector. n_{fill} was computed here for each edge detector so that the number of 1's accepted was equivalent to the same fraction of the edge region as was used in [1].

The definitions of the two edge detection performance parameters were generalized to apply to the thresholded edge detector output described above in a straightforward manner. Effectively, the only difference in the form of the thresholded output between non-vertical edges and vertical edges is that the corners of output from test images with non-vertical edges were'rotated out'. Consequently, to generalize the definition of parameter 1, it was necessary only to reexpress it in such a manner that it was no longer implicitly assumed that the output domain was rectangular. Parameter 2 depended on the edge region being rectangular, but the'rotated-out'corners in some cases extended into the edge region. When this occurred, the rows of the edge region which were missing points were excluded from the computation of parameter 2.

The expressions for the two parameters may now be given. Let n_{tot} be the total number of points in the rotated-back edge detector output, n_{in} the number of such points in the edge region and n_{out}, the number of such points outside the edge region ($n_{tot} = n_{in} + n_{out}$). Define $n^o(n^e)$, as in [1], as the number of ones in the thresholded edge detector output outside (inside) the edge region and let w_1^e be the number of columns contained in the rotated-back edge region. Finally let f be a standard fraction of the rotated-back thresholded edge detector output taken up by the edge region. It was necessary to normalize the edge detector output to a standard proportion of edge region versus non-edge region so as not to bias the results in favor of outputs in which the edge region occupied a greater fraction of the total points. In [1], the function of standardizing the fraction of the output taken up by the edge region was performed by w_1^{stan}, the number of columns of a standard output size. There w_1^{stan} was 30 columns and the edge region consisted of 6 columns. Here, f was set equal to .2 in order to keep the same proportions. Here also the edge region occupied 6 columns.

The formulae used to compute the two edge detection performance parameters were as follows. Parameter 1 was given by

$$P_1 = \frac{n^e_{sig}}{n^e_{sig} + (n^e_{noise} + n^o)\frac{n_{in}}{fn_{tot}}}$$

where

$$n^e_{sig} = \frac{n^e - n^e_{noise}}{1 - \frac{n^e_{noise}}{n_{in}}}$$

and

$$n^e_{noise} = n^o \frac{n_{in}}{n_{out}}$$

The significance of n^e_{noise} can be understood in the context of the model used in [1]. Under this model, it is assumed, first, that in the thresholded edge detector output the only 1's present outside the edge region are due to noise, and secondly, that the "noise" 1's are distributed randomly throughout this output. n^e_{noise} is an estimate of the number of noise 1's inside the edge region. In this model, the number of 1's in the edge region due only to signal is then estimated by $n^e - n^e_{noise}$ and n^e_{sig} is an estimate of the total number of signal 1's in the edge region. (Some of the 1's in the edge region according to this model are due both to signal and noise).

Let n_r be the number of rows of the rotated-back thresholded edge detector output which contain at least one 1. Let w_1^e be the number of columns in the edge region of this output and let w_2 be the number of rows contained in the largest rectangle which can be inscribed in the edge region. Then parameter 2 is given by

$$P_2 = \frac{\frac{n_r}{w_r} - \left\{1 - \left[1 - \frac{n^e_{noise}}{n_{in}}\right]^{w_1^e}\right\}}{\left[1 - \frac{n^e_{noise}}{n_{in}}\right]^{w_1^e}}$$

This formula may also be understood in the context of the model described above. $\frac{n_r}{w_r}$ is the fraction of rows of the edge region which contain at least one 1. $\left[1 - \frac{n^e_{noise}}{n_{in}}\right]^{w_1^e}$ is an estimate of the fraction of rows of the edge region which contain no noise 1's. Therefore $1 - \left[1 - \frac{n^e_{noise}}{n_{in}}\right]^{w_1^e}$ is the corresponding estimate of the fraction of rows of this region which contain at least one noise 1, and parameter 2 is an estimate of the ratio of the number of "edge" rows which contain at least one signal 1 and no noise 1's divided by the total number of "edge" rows which contain no noise 1's.

3.3 Results.

The results of the tests described in the previous paragraph are tabulated in Table 2 and plotted in Figures 2-4.

It can be seen that within statistical fluctuations, the changes in the rated performance of the edge detection schemes with orientation and contrast-to-noise ratios is consistent with what one would expect on general principles. The performance of Hueckel's operator is roughly independent of the orientation of the test edges, and the performance of the other schemes falls off as the orientation of the test images becomes farther from the ideal orientation(s). This falloff is most pronounced at the intermediate contrast-to-noise ratios. That is to say, if an edge is very distinct, then it can be detected over a wide range of orientations. If the edge is not very distinct, then the range of orientations in which it can be detected is smaller.

It can be seen in Figures 2 and 3 that the parameter 1 rating of the 2-orientation implementation of Rosenfeld's scheme is generally lower than the 1-orientation implementation. There are two effects which can explain this discrepanyc. First, the 2-orientation implementation included non-maximum suppression. This operation is useful for compressing the information of the edge detector output, but it can be expected to compress the noise less than it compresses the signal. Secondly, for near-vertical test edges, the addition of the second optimum orientation could be expected only to add noise. The addition of the second optimum orientation

should not be expected to alter the signal-to-noise ratio of the output for test edges oriented at 45° to the vertical, however, since the output from each optimum orientation should be about the same there. One would expect an improvement in the performance of the 2-orientation implementation from 45° to 60°, however, and this is consistently evidenced in the data.

An interesting result of this study in comparing the two implementations of Rosenfeld's scheme can be seen clearly in Figures 4(h) - 4(j). There, the test edges were so distinct that no orientation bias could be detected in the 1-orientation implementation. The 2-orientation implementation, however, exhibits this bias. While its parameter 2 rating for vertical edges is essentially ideal, this rating falls off for skew edges. It seems likely, therefore, that the non-maximum suppression algorithm used in the 2-orientation implementation introduces an angular bias.

It can be seen in Figures 3 and 4 that the method of Macleod as programmed here is much more biased with respect to the orientation of the test edges than the method due to Rosenfeld. A likely explanation for this is the shape of the mask used in implementing Macleod's scheme. One would expect a square-shaped mask to be more sensitive to orientation than an elongated one. Effectively, the mask used in

Rosenfeld's scheme was elongated since it consisted of two squares next to each other. The selection of a square-shaped mask for Macleod's scheme, however, was no an inherent feature of the method, but an arbitrary choice of the investigators.

4. CONCLUDING REMARKS - A COMPARISON WITH ANOTHER METHOD OF QUANTIFYING EDGE DETECTOR PERFORMANCE

The only other attempt known to the investigators to quantify edge detection performance was that of Herskovits [8]. The quantification methods of [8] are easily interpretable but they are hard to apply to most edge detection schemes. In contrast, while the exact meaning of the two parameters calculated here is admittedly open to discussion, they can be estimated easily for a wide range of edge detection schemes. It is clear that our parameters in some sense reflect the quality of edge detection, but a comparison with the more straightforward approach of Herskovits is useful.

The most obvious method of comparing the quantification methods in [8] with those of this work would seem to be to calculate the two parameters used here for the principal edge detection method suggested in [8], the computation of F_{step}. Unfortunately, this could not be done on the test images used here because all but eight columns of the edge detector output would be lost to the margins leaving only two columns of non-edge region. Consequently, the set of test images specified in Table 3 was generated for the purposes of rating Herskovits' scheme with the parameters of this work. The noise level of these test images, 12 grey level units, was chosen because it is small in comparison to our total grey level

scale (64), and its conversion to the vidlog units of [8] is convenient. The noise level assumed in [8] was 1.2 vidlog units making the conversion of grey level units to vidlog units 10 to 1.

The function F_{step} was calculated over the set of test images specified in Table 3 using the optimum parameters determined in [8]--that is a neighborhood size of 70, a second difference cutoff of 1 vidlog unit (10 grey level units), an S cutoff of 14 and an F_{step} threshold of 16. The resulting determinations of the two parameters of this work are plotted in Figure 6. The solid line of Figure 6 is taken from Figure 24 in [8]. It is the "global detection characteristic" of F_{step}, the probability that a straight edge could be recognized on the basis of the calculation of F_{step} over five bands along its length using a simple algorithm suggested by Herskovits.

It can be seen from Figure 6 that parameter 2 forms an alternative indicator of edge detection performance to that of Herskovits in the sense that it varies from a null rating to an ideal rating over roughly the same ratios of contrast to noise. The agreement between parameter 1 and Herskovits' 'global detection characteristic' is not as good for the higher contrast-to-noise ratios. This agreement could be made better

if the cutoff points, rather than all points for which F_{step} exceeded threshold (local maxima) were stored as in [8], and the "parasite extrema" were removed as was also done in [8]. In addition, the edge region could have been made larger. Only the two columns adjacent to the step edge were used here.

5. REFERENCES

[1] Fram, J. R., and Deutsch, E.S., "On the Quantitative Evaluation of Edge Detection Schemes and their Comparison with Human Performance", University of Maryland Technical Report No. 73-221, March 1973.

[2] Meurle, J. L., and Allen, D. C., "Experimental Evaluation of Techniques for Automatic Segmentation of Objects in a Complex Scene", in Pictorial Pattern Recognition, Cheng, G. C., et al, eds., Thompson Book Co., Washington, D. C. 1968.

[3] Meurle, J. L., Private communication.

[4] Gupta, J. N. et al, "Machine Boundary Findings and Sample Classification of Remotely Sensed Agricultural Data", Proc. Conf. on Machine Processing of Remotely Sensed Data, October 16-18, 1973, IEEE Catalog No. 73 CHO 834-2GE.

[5] Hueckel, M., "A Local Visual Operator Which Recognizes Edges and Lines", JACM 20, 4, 634, October 1973.

[6] Macleod, I.D.G., "On Finding Structure in Pictures", Picture Language Machines, S. Kaneff, ed., Academic Press, New York, 1970, p. 231.
See also Macleod, I.D.G., "Comments on 'Techniques for Edge Detection'", Proc. IEEE, 60, p. 344, 1972.

[7] Rosenfeld, A., Thurston, M., "Edge and Curve Detection for Visual Scene Analysis", IEEE Trans., C-20, May 1971.

[8] Herskovits, A., and Binford, T. O., "On Boundary Detection", MIT Project MAC Artificial Intelligence Memo No. 183, July 1970.

[9] This method of determining a threshold, the "p-tile method", is discussed in Rosenfeld, A., "Picture Processing by Computer", Academic Press, New York, 1969, p. 132.
The specifics of its implementation here are discussed in [1], Section 3.1.

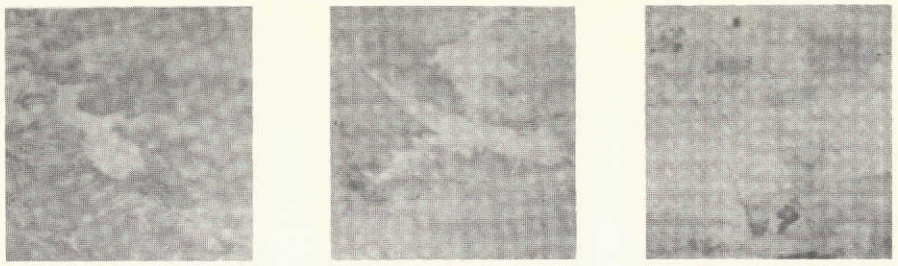

Originals

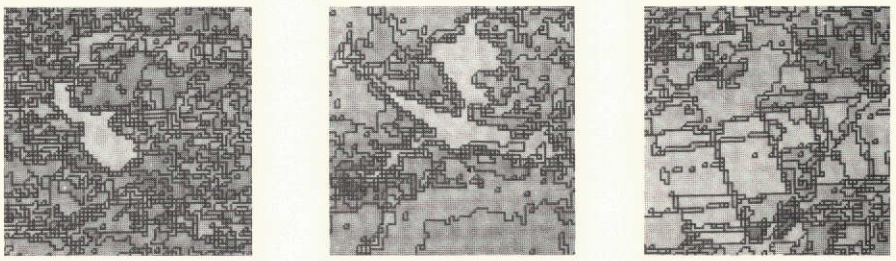

d=2, μ=2

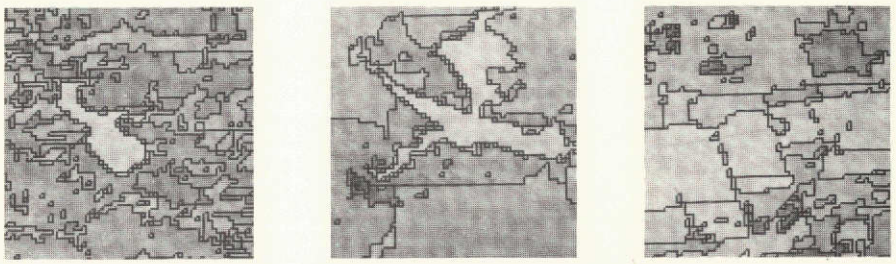

d=2, μ=4

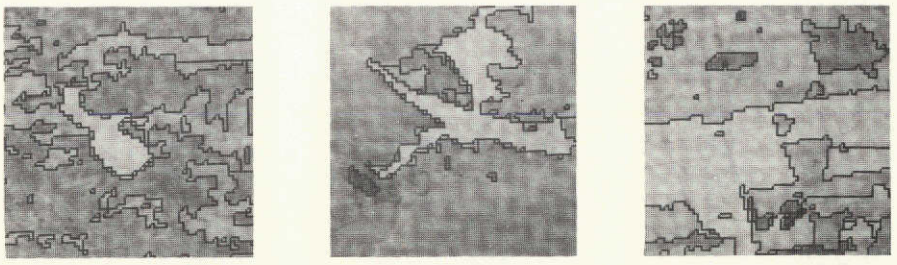

d=2, μ=6

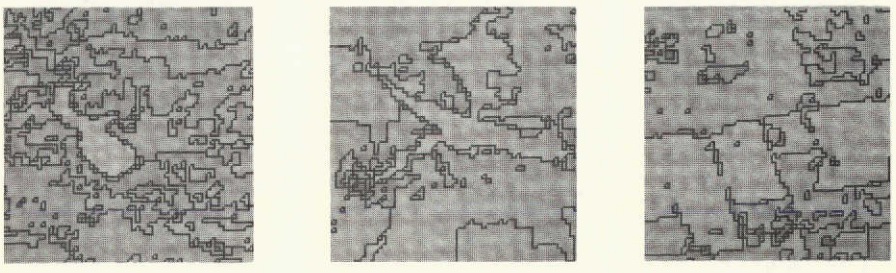

d=4, μ=2

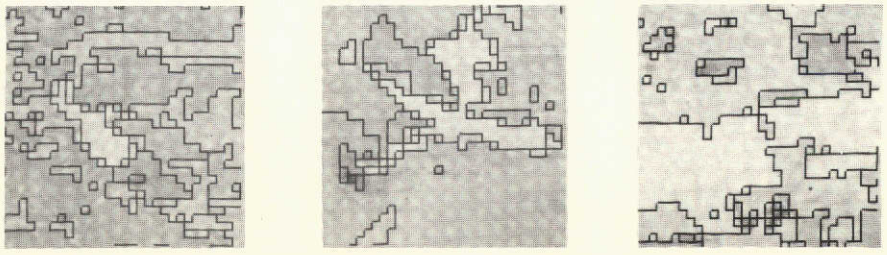

d=4, μ=4

Figure 1

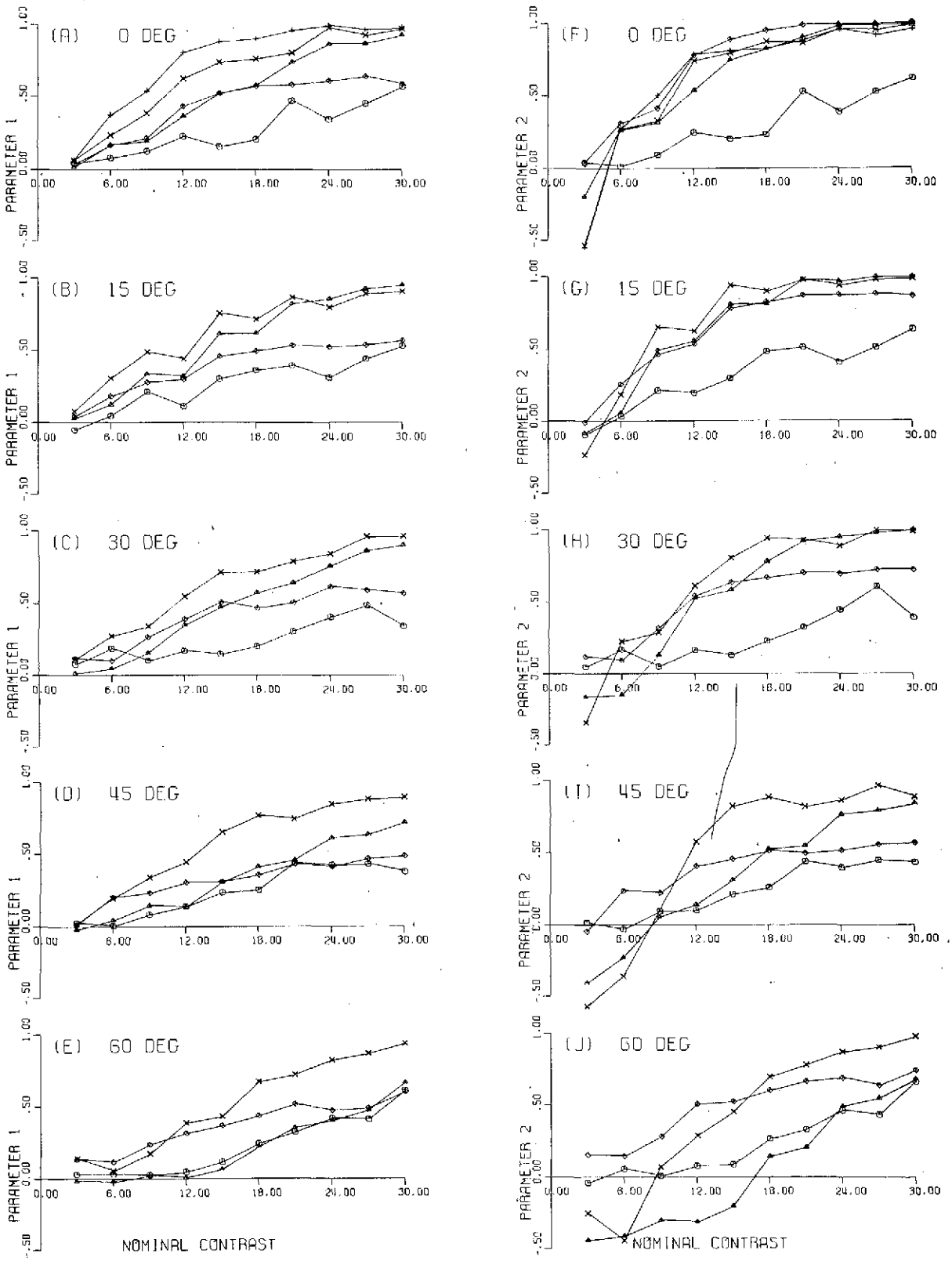
(A) 0 DEG
(B) 15 DEG
(C) 30 DEG
(D) 45 DEG
(E) 60 DEG
(F) 0 DEG
(G) 15 DEG
(H) 30 DEG
(I) 45 DEG
(J) 60 DEG
PARAMETER 1
PARAMETER 2
NOMINAL CONTRAST
HUECKEL
MCLD SMALL
MCLD LARGE
ROS 1 ORIENT
ROS 2 ORIENT

FIG. 3

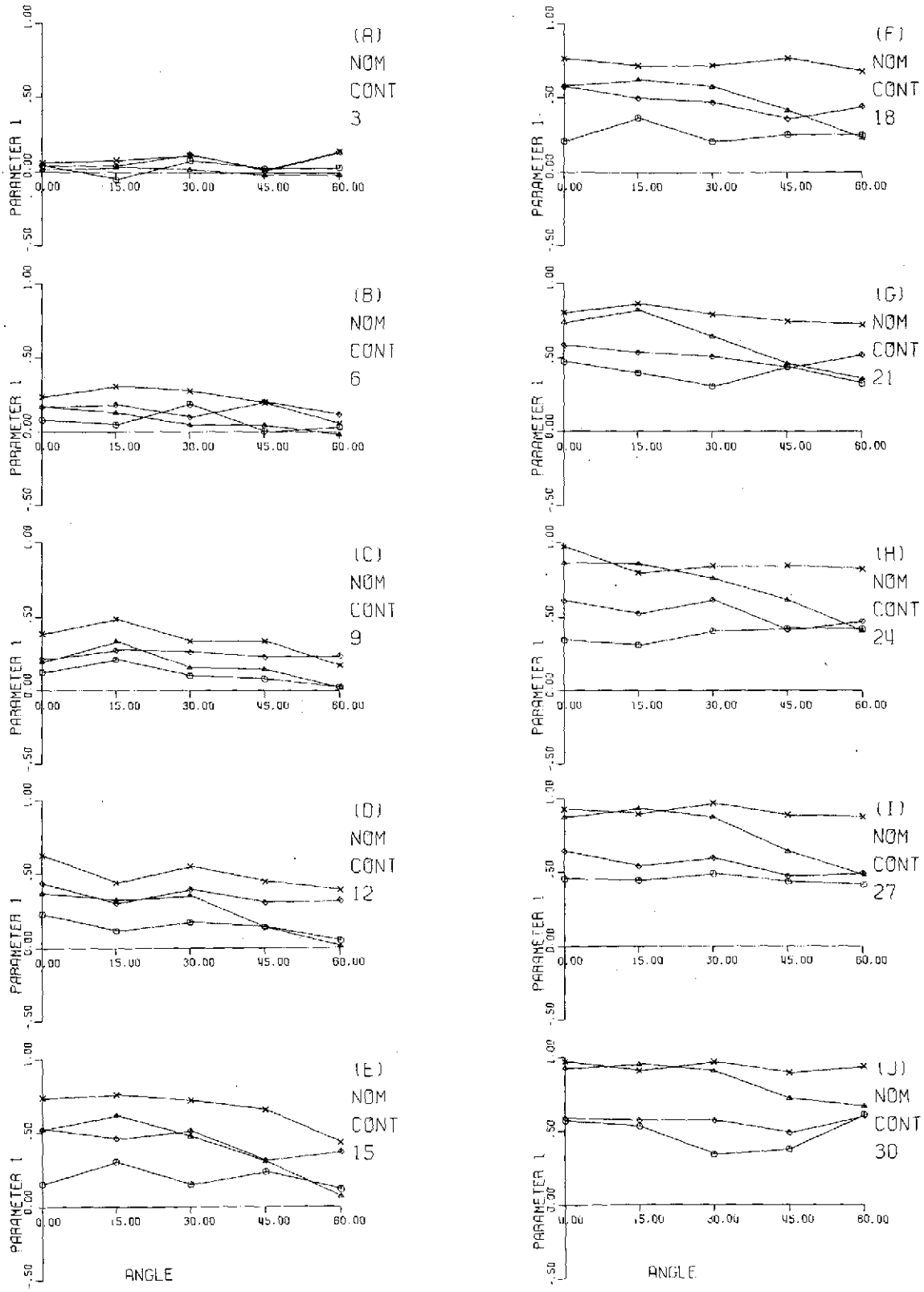
(A)
NOM
CONT
3
(B)
NOM
CONT
6
(C)
NOM
CONT
9
(D)
NOM
CONT
12
(E)
NOM
CONT
15
(F)
NOM
CONT
18
(G)
NOM
CONT
21
(H)
NOM
CONT
24
(I)
NOM
CONT
27
(J)
NOM
CONT
30
PARAMETER 1
1.00
.50
0.00
-.50
0.00
15.00
30.00
45.00
60.00
ANGLE
HUECKEL
MOLO SMALL
ROS 1 ORIENT
ROS 2 ORIENT

FIG. 4

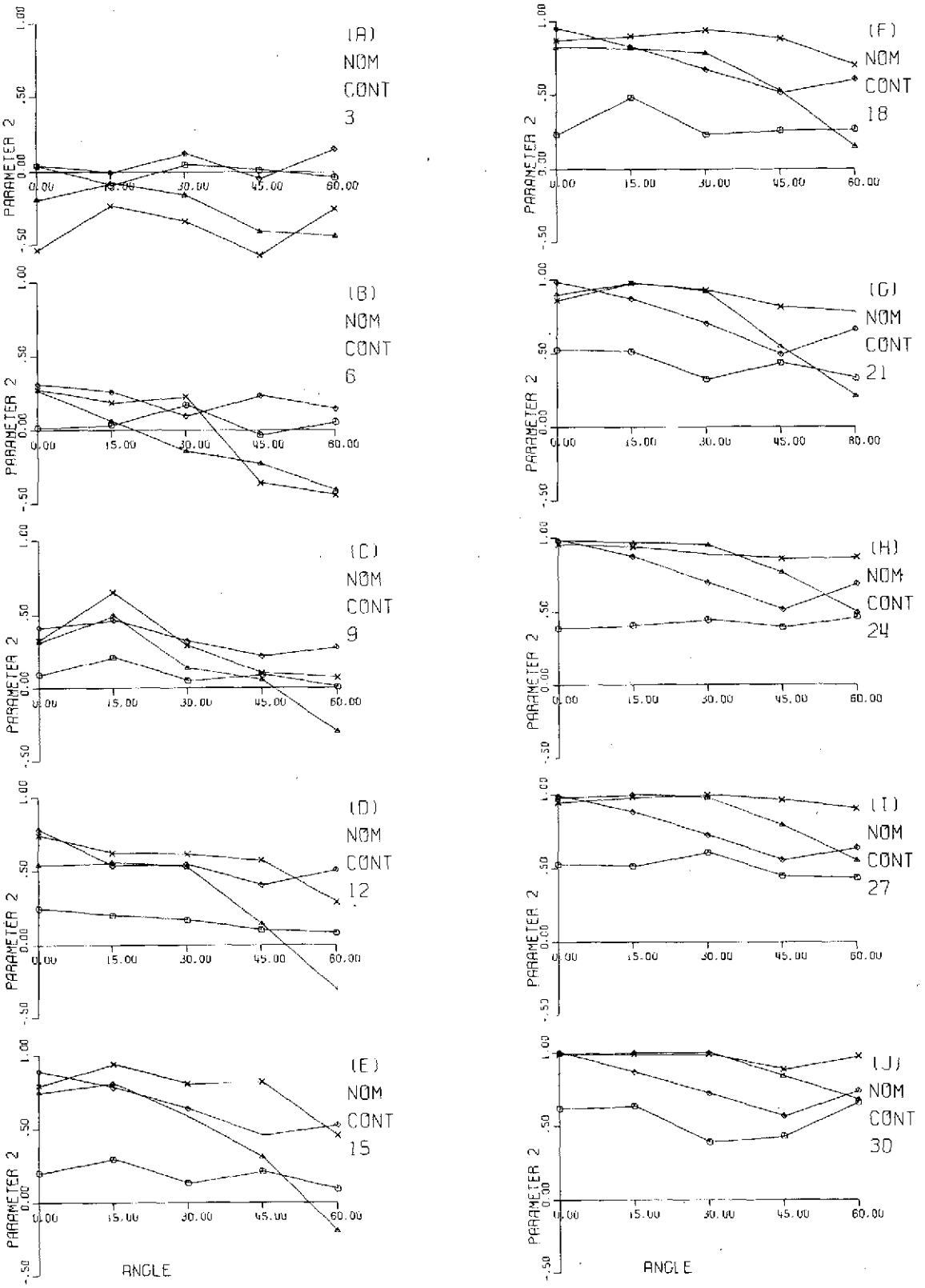
(A)
NOM
CONT
3
(B)
NOM
CONT
6
(C)
NOM
CONT
9
(D)
NOM
CONT
12
(E)
NOM
CONT
15
(F)
NOM
CONT
18
(G)
NOM
CONT
21
(H)
NOM
CONT
24
(I)
NOM
CONT
27
(J)
NOM
CONT
30
PARAMETER 2
ANGLE
0.00
15.00
30.00
45.00
60.00
1.00
.50
0.00
-.50
HUECKEL
MOLD SMALL
ROS 1 ORIENT
ROS 2 ORIENT

FIG. 5

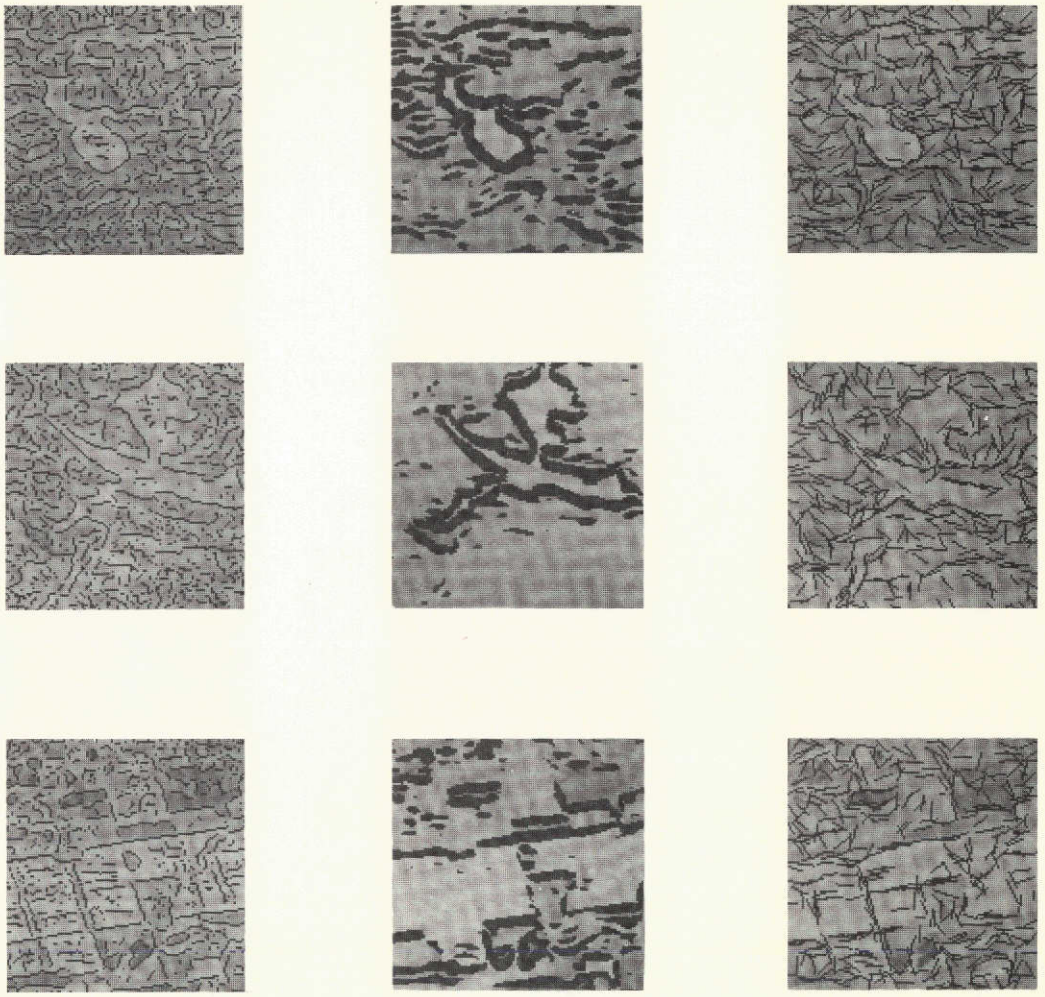

Rosenfeld
(Threshold = 1)

Macleod
(Threshold = 20)

Hueckel

Figure 2.

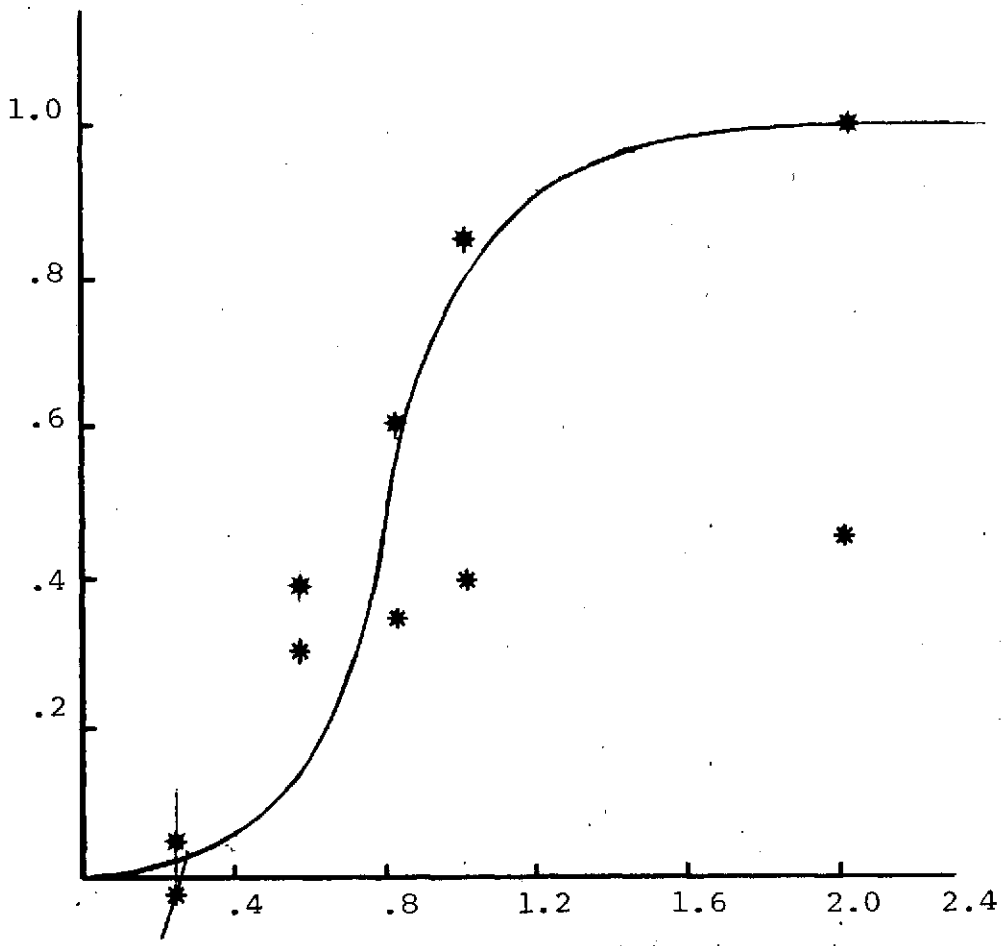
1.0
.8
.6
.4
.2
.4
.8
1.2
1.6
2.0
2.4
signal in number of light intensity
standard-deviations
parameter 1
parameter 2
Herskovits' global detection characteristic

Figure 6.

g_1	g_2	NOMINAL CONTRAST	NOMINAL NOISE	ACTUAL CONTRAST	ACTUAL NOISE	NO. OF PICTURES AT EACH ORIENTATION
30	33	3	24	1.4	16.4	10
29	35	6	24	2.8	16.3	10
27	36	9	24	4.2	16.3	10
26	38	12	24	5.6	16.2	10
24	39	15	24	6.9	16.2	10
23	41	18	24	8.3	16.1	10
21	42	21	24	9.6	16.0	10
20	44	24	24	11.0	15.9	10
18	45	27	24	12.3	15.8	10
17	47	20	24	13.6	15.7	7 at 0° 10 at others

Table 1. Parameters of the set of test images. The edge orientations were 0°, 15°, 30°, 45° and 60°. The makeup of the vertical edge (0°) test images is described fully in [1]. The other orientations were produced by rotating the vertical edge test images.

ANGLE	NOMINAL CONTRAST									
	3	6	9	12	15	18	21	24	27	30
0	.04+-.05	.08+-.07	.12+-.06	.22+-.05	.15+-.06	.20+-.04	.47+-.07	.34+-.05	.45+-.07	.57+-.12
15	-.05+-.03	.05+-.07	.21+-.07	.11+-.05	.30+-.07	.36+-.07	.39+-.06	.31+-.05	.44+-.07	.53+-.04
30	.07+-.06	.19+-.05	.10+-.05	.17+-.07	.15+-.06	.20+-.08	.30+-.10	.40+-.09	.48+-.06	.34+-.07
45	.02+-.04	.00+-.05	.08+-.07	.13+-.07	.23+-.07	.25+-.05	.43+-.07	.42+-.04	.43+-.08	.38+-.09
60	.03+-.07	.03+-.06	.02+-.05	.04+-.06	.11+-.02	.24+-.07	.32+-.09	.42+-.05	.41+-.09	.61+-.05

Table 2(a). Hueckel edge detector parameter 1.

ANGLE	NOMINAL CONTRAST									
	3	6	9	12	15	18	21	24	27	30
0	.03+-.08	.01+-.09	.09+-.07	.24+-.05	.20+-.07	.23+-.05	.52+-.07	.38+-.06	.52+-.07	.62+-.11
15	-.10+-.04	.03+-.09	.21+-.08	.20+-.08	.30+-.07	.48+-.09	.51+-.07	.40+-.07	.51+-.06	.63+-.03
30	.04+-.07	.17+-.07	.05+-.05	.16+-.07	.13+-.06	.23+-.06	.32+-.10	.44+-.08	.60+-.07	.39+-.09
45	.01+-.05	-.04+-.06	.09+-.10	.09+-.07	.21+-.09	.25+-.05	.43+-.07	.39+-.03	.44+-.06	.43+-.08
60	-.04+-.07	.05+-.07	.00+-.05	.07+-.06	.09+-.04	.26+-.07	.33+-.09	.46+-.05	.43+-.10	.66+-.05

Table 2(b). Hueckel edge detector parameter 2.

ANGLE	NOMINAL CONTRAST									
	3	6	9	12	15	18	21	24	27	30
0	.06+-.09	.37+-.10	.54+-.08	.80+-.06	.88+-.03	.90+-.02	.96+-.02	.99+-.00	.96+-.02	.98+-.02

Table 2(c). Macleod large edge detector parameter 1.

EDGE DETECTOR "B PARAMETER 2

ANGLE	NOMINAL CONTRAST									
	3	6	9	12	15	18	21	24	27	30
0	-.55+-.29	.27+-.18	.50+-.10	.78+-.07	.81+-.03	.82+-.04	.88+-.03	.95+-.03	.91+-.04	.96+-.03

Table 2(d). Macleod large edge detector parameter 2.

ANGLE	NOMINAL CONTRAST 3	6	9	12	15	18	21	24	27	30
0	.01+-.04	.16+-.04	.19+-.03	.36+-.04	.52+-.04	.58+-.04	.74+-.04	.86+-.03	.87+-.02	.92+-.01
15	.03+-.03	.12+-.05	.34+-.05	.32+-.03	.61+-.04	.62+-.03	.82+-.03	.86+-.03	.93+-.01	.95+-.02
30	.01+-.03	.04+-.03	.16+-.04	.35+-.03	.47+-.04	.57+-.03	.64+-.03	.76+-.03	.86+-.04	.90+-.01
45	-.02+-.05	.04+-.05	.14+-.05	.13+-.04	.30+-.06	.41+-.05	.45+-.04	.61+-.03	.63+-.04	.71+-.03
60	-.02+-.03	-.02+-.05	.02+-.04	.01+-.04	.07+-.05	.22+-.03	.35+-.04	.40+-.02	.47+-.04	.66+-.03

Table 2(e). Macleod small edge detector parameter 1.

ANGLE	NOMINAL CONTRAST 3	6	9	12	15	18	21	24	27	30
0	-.20+-.11	.26+-.12	.31+-.07	.54+-.06	.74+-.06	.82+-.04	.90+-.03	.98+-.02	.98+-.01	.99+-.01
15	-.08+-.11	.06+-.13	.49+-.08	.56+-.05	.81+-.04	.81+-.04	.98+-.01	.97+-.01	1.00+-.00	1.00+-.00
30	-.18+-.07	-.15+-.06	.13+-.09	.52+-.08	.58+-.08	.78+-.04	.92+-.02	.95+-.02	.98+-.02	1.00+-.00
45	-.41+-.15	-.23+-.13	.05+-.11	.14+-.08	.30+-.07	.52+-.06	.54+-.05	.76+-.05	.79+-.04	.84+-.04
60	-.44+-.12	-.41+-.15	-.30+-.12	-.31+-.10	-.20+-.11	.14+-.07	.20+-.07	.49+-.06	.55+-.06	.68+-.04

Table 2(f). Macleod small edge detector parameter 2.

ANGLE	NOMINAL CONTRAST 3	6	9	12	15	18	21	24	27	30
0	.06+-.06	.23+-.05	.39+-.06	.62+-.05	.74+-.03	.76+-.04	.80+-.04	.97+-.01	.92+-.02	.97+-.02
15	.08+-.05	.31+-.07	.49+-.06	.44+-.05	.76+-.03	.71+-.04	.87+-.03	.80+-.04	.89+-.01	.90+-.02
30	.11+-.06	.27+-.05	.34+-.06	.55+-.06	.71+-.06	.72+-.04	.79+-.04	.84+-.04	.96+-.01	.96+-.01
45	.01+-.04	.19+-.08	.34+-.08	.44+-.04	.65+-.06	.77+-.05	.74+-.05	.84+-.05	.88+-.03	.89+-.04
60	.14+-.05	.05+-.03	.17+-.04	.39+-.07	.43+-.05	.67+-.07	.72+-.04	.82+-.04	.87+-.04	.93+-.02

Table 2(g). Rosenfeld 1-orientation edge detector parameter 1.

ANGLE	NOMINAL CONTRAST 3	6	9	12	15	18	21	24	27	30
0	-.54+-.39	.27+-.17	.32+-.15	.74+-.06	.79+-.04	.87+-.03	.86+-.04	.95+-.02	.95+-.03	.99+-.01
15	-.23+-.23	.18+-.21	.65+-.09	.62+-.06	.94+-.03	.90+-.04	.98+-.01	.94+-.03	.98+-.01	.98+-.02
30	-.34+-.18	.22+-.12	.29+-.15	.61+-.10	.80+-.04	.94+-.02	.93+-.02	.89+-.04	.99+-.01	.98+-.01
45	-.57+-.26	-.36+-.46	.10+-.36	.57+-.09	.82+-.04	.88+-.05	.81+-.04	.86+-.09	.96+-.02	.88+-.04
60	-.25+-.18	-.44+-.16	.07+-.13	.29+-.20	.45+-.11	.69+-.09	.78+-.07	.87+-.05	.90+-.05	.97+-.01

Table 2(h). Rosenfeld 1-orientation edge detector parameter 2.

ANGLE	NOMINAL CONTRAST									
	3	6	9	12	15	18	21	24	27	30
0	.03+-.03	.16+-.03	.21+-.07	.43+-.04	.52+-.04	.57+-.04	.58+-.02	.61+-.02	.64+-.03	.58+-.01
15	.04+-.03	.13+-.07	.28+-.06	.30+-.04	.46+-.03	.49+-.04	.53+-.05	.52+-.03	.54+-.02	.57+-.04
30	.11+-.05	.10+-.05	.26+-.06	.39+-.06	.51+-.04	.46+-.02	.50+-.04	.61+-.05	.59+-.05	.57+-.04
45	.01+-.05	.20+-.07	.23+-.08	.30+-.04	.31+-.03	.35+-.05	.43+-.05	.41+-.04	.47+-.05	.48+-.06
60	.13+-.05	.12+-.06	.24+-.06	.31+-.04	.37+-.04	.43+-.03	.51+-.05	.47+-.04	.49+-.05	.60+-.05

Table 2(i). Rosenfeld 2-orientation edge detector parameter 1.

ANGLE	NOMINAL CONTRAST									
	3	6	9	12	15	18	21	24	27	30
0	.04+-.08	.31+-.05	.41+-.13	.78+-.05	.89+-.05	.95+-.03	.98+-.01	.98+-.02	.99+-.01	1.00+-.00
15	-.01+-.07	.26+-.11	.46+-.10	.53+-.07	.78+-.04	.82+-.04	.87+-.03	.87+-.01	.88+-.01	.86+-.02
30	.12+-.06	.09+-.08	.32+-.08	.54+-.07	.63+-.04	.67+-.02	.70+-.04	.69+-.04	.72+-.04	.72+-.02
45	-.05+-.09	.23+-.12	.22+-.11	.40+-.03	.45+-.03	.51+-.05	.49+-.04	.51+-.04	.55+-.03	.56+-.03
60	.15+-.05	.14+-.07	.28+-.08	.51+-.07	.52+-.05	.60+-.04	.66+-.05	.69+-.04	.64+-.03	.74+-.02

Table 2(j). Rosenfeld 2-orientation edge detector parameter 2.

g_1	g_2	NOMINAL CONTRAST	NOMINAL NOISE	NUMBER OF PICTURES
30	33	3	12	10
29	36	7	12	65
27	37	10	12	100
25	38	13	12	65
19	44	25	12	10

Table 3. The test images used for a comparison with Herskovits' method of qunatifying edge detector performance. The test images all contained vertical step edges with gaussian noise of standard deviation 12. See [1] for further details.